International Journal of Thermophysics, Vol. 27, No. 1, January 2006 (© 2006)
DOI: 10.1007/s10765-006-0032-7

Two Effective Thermal Conductivity Models for Porous Media with Hollow Spherical Agglomerates[1]

Fan Yu,[2] Gaosheng Wei,[2] Xinxin Zhang,[2,3] and Kui Chen[2]

Based on the microstructure features of xonotlite-type micro-pore calcium silicate, two unit cell models, the point-contact hollow spherical model and the surface-contact hollow cubic model, are developed. As one of several excellent insulation materials, xonotlite is represented as porous media with hollow spherical agglomerates. By one-dimensional heat conduction analysis using the unit cell, the effective thermal conductivity of xonotlite is determined. The results show that both of the models are in agreement with experimental data. The algebraic expressions based on the unit cell models can be used to calculate the effective thermal conductivity of porous media that have similar structure features as xonotlite.

KEY WORDS: calcium silicate; insulation; thermal conductivity; xonotlite.

1. INTRODUCTION

Some high efficiency composite insulation materials based on the theory of self-assembly for nanostructured materials have appeared in recent years, such as adiabatic tiles using fire-retardant fibers compounded with silica aerogel, which have been used in an insulation layer on space shuttles [1]. Compared with fire-retardant fiber, xonotlite provides better insulating performance, which has been emphasized in recent years in several studies [2–4]. Silica aerogel has very low thermal conductivity but is brittle. It is expected to provide even better insulation performance by compounding

[1] Paper presented at the Seventh Asian Thermophysical Properties Conference, August 23–28, 2004, Hefei and Huangshan, Anhui, P. R. China

[2] Department of Thermal Engineering, University of Science and Technology Beijing, Beijing 100083, P. R. China

[3] To whom correspondence should be addressed. E-mail: xxzhang@ustb.edu.cn

xonotlite with silica aerogel. Due to the nano-pores in this composite material, its thermal conductivity can be very low (lower than non-convective air) [5]. The extreme adiabatic capability results in these materials having very high application potential in the heat protection of space shuttles, nuke reactors, and even ordinary steam pipes. The effective thermal conductivity is the key parameter for evaluating the performance of these insulation materials. The development of an effective thermal conductivity model based on the material's microstructure is extremely important for the thermal design and analysis of xonotlite and xonotlite-aerogel composite insulation materials.

Heat transfer models in porous insulation materials must describe heat transfer mechanisms such as solid conduction, gas conduction, and radiation through participating media. Natural convection can always be neglected if the pores in the material are small (< 4 mm) [6]. In the past, many studies have resulted in various theoretical models to estimate the effective thermal conductivity of porous media with different geometrical structures, such as Russell, Eucken and Loeb models [7] based on cylindrical or spherical pore structures. Zehnder and Schlunder [8] proposed a correlation for the stagnant thermal conductivity based on a one-dimensional heat flow model for heat conduction through a packed bed of spherical particles. Zimmerman [9] presented a thermal conductivity model for fluid-saturated rocks by using an effective medium theory. Verma et al. [10] developed an expression for predicting the effective thermal conductivity with spherical inclusions. Hsu et al. [11] developed a lumped-parameter model for the effective stagnant thermal conductivity of some two-dimensional and three-dimensional spatially periodic media. Yu and Cheng [12] developed a fractal thermal conductivity model for both mono- and bi-dispersed porous media by assuming that porous media consist of two parts: some particles contact each other to form tortuous chains, whereas others do not touch each other. More recently, Ma et al. [13] have developed a self-similarity model for the effective thermal conductivity of porous media based on the thermal–electrical analogy technique and on the statistical self-similarity existing in porous media. As the model of Ma et al. may be only applicable to the porosity range of about 0.3 to 0.5, Feng et al. [14] extended the work of Ma et al. to a generalized model to cover a wide range of porosity of 0.14–0.80. All these models have limited applicability and none correctly predict the thermal conductivity of xonotlite insulation material with a porosity as high as 90%.

In this paper, by analyzing the microstructure of xonotlite, two effective thermal conductivity models, the point-contact hollow spherical model and the surface-contact hollow cubic model, are developed for the coupled conduction in high porosity materials.

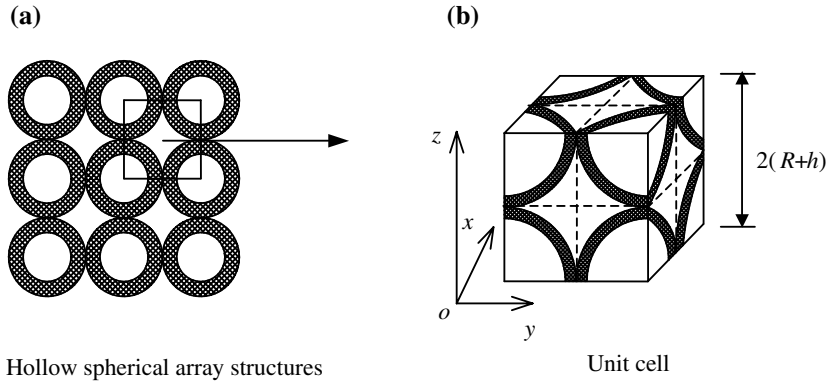

Fig. 1. Simplified microstructures and unit cell model of xonotlite. (a) Hollow spherical array structures and (b) Unit cell.

2. POINT-CONTACT HOLLOW SPHERICAL MODEL

2.1. Geometrical Structure

Using a scanning electron microscope image of xonotlite, we find that xonotlite is made up of hollow spherical agglomerates interwoven with xonotlite fibers with radii from hundreds to thousands of nanometers. By simplification, xonotlite is considered as a periodical array of hollow spheres with an inner radius R and shell thickness h, as shown in Fig. 1a. All of the hollow spheres are in point contact.

Since the shell consists of xonotlite fibers, there exist pores in it. If the porosity of the shell is Φ_{i}, the total porosity of the unit cell, as shown in Fig. 1b is

$$\Phi = 1 - \frac{\pi}{6}(1 - \Phi_i)\left[1 - \left(\frac{R}{R+h}\right)^3\right] \tag{1}$$

2.2. Effective Thermal Conductivity

First, radiation heat transfer is not considered. Assume that one-dimensional heat transfer occurs along the opposite z axis. Based on the symmetry of the structure, the unit cell can be divided into two parts: one is the coherent fluid at the center part, and the other is a quarter of column with a radius $(R + h)$, which also includes two parts, as shown in Fig. 2. The effective thermal conductivity of the unit cell is

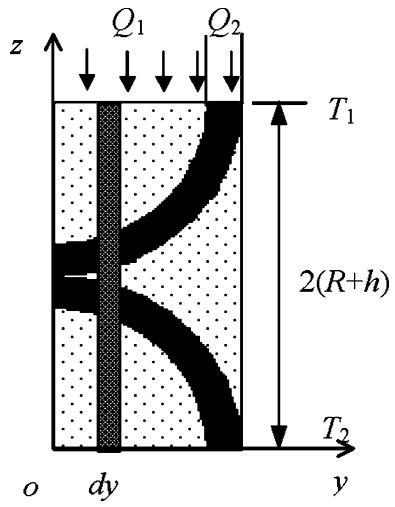

Fig. 2. Heat transfer analysis in the unit cell.

$$k_e = \left(1 - \frac{\pi}{4}\right) k_f + \frac{\pi}{4} k_{sf} \tag{2}$$

where k_f is the thermal conductivity of the fluid and k_{sf} is the effective thermal conductivity of a quarter of a column. As shown in Fig. 2, T_1 and T_2 are the temperatures of the top and bottom surfaces, respectively. Heat conduction in the structure consists of two parts: Q_1, through a quarter of a column with radius R, and Q_2, through a quarter of a hollow cylinder with a thickness h. According to Fourier's law, the expressions for Q_1 and Q_2 are

$$Q_1 = \frac{(T_1 - T_2)k_f}{4} \int_0^R \frac{\pi y \, dy}{(R+h) - \beta(\sqrt{(R+h)^2 - y^2} - \sqrt{R^2 - y^2})} \tag{3}$$

$$Q_2 = \frac{(T_1 - T_2)k_f}{4} \int_R^{R+h} \frac{\pi y \, dy}{R + h - \beta\sqrt{(R+h)^2 - y^2}} \tag{4}$$

Here, $\beta = 1 - k_f / k_c$, where k_c is the thermal conductivity of the shell and k_f is the thermal conductivity of the fluid. Integrating Eq. (3) and (4), have

$$Q_1 = \frac{k_g \pi \Delta T}{16\alpha}\left[\frac{\alpha^4(2Rh+h^2)^2-(R+h)^4}{\alpha(R+h)^3}\ln\sqrt{\frac{2R+h}{h}}\cdot\frac{(R+h-\alpha h)}{(R+h-\alpha\sqrt{2Rh+h^2})}\right.$$
$$+\frac{\alpha R(2R+h)(R+h)+\alpha^2 h(2R+h)^2-(R+h)^2 h-\alpha^2 h(2R+h)\sqrt{2Rh+h^2}}{(R+h)^2}$$
$$\left.+\sqrt{2Rh+h^2}+\frac{(R+h)}{\alpha}\ln\sqrt{\frac{2R+h}{h}}\right] \tag{5}$$

$$Q_2 = \frac{k_g \pi \Delta T}{4\alpha}\left[\frac{R+h}{\alpha} ln\left(\frac{R+h}{R+h-\alpha\sqrt{2Rh+h^2}}\right)-\sqrt{2Rh+h^2}\right] \tag{6}$$

The effective thermal conductivity k_{sf} is given by

$$k_{sf} = \frac{2(R+h)(Q_1+Q_2)}{\frac{1}{4}\pi(R+h)^2\Delta T} = \frac{8(Q_1+Q_2)}{\pi(R+h)\Delta T} \tag{7}$$

Substituting Eqs. (5) and (6) into Eq. (7) and considering Eq. (1), we get

$$k_{sf} = \frac{k_f}{2}\left\{A(1+A)+(1-A^2)(1+A-\sqrt{1-A^2})\beta-(1-A+3\sqrt{1-A^2})\frac{1}{\beta}\right.$$
$$\left.-\frac{1}{\beta^2}\ln[(1-\beta+\beta A)(1-\beta\sqrt{1-A^2})^3]+\beta^2(1-A^2)^2\ln\left[\sqrt{\frac{1+A}{1-A}}\frac{1-\beta(1-A)}{1-\beta\sqrt{1-A^2}}\right]\right\} \tag{8}$$

Here,

$$A = \sqrt[3]{1-\frac{6}{\pi}\left(\frac{1-\Phi}{1-\Phi_i}\right)} \tag{9}$$

Substituting Eq. (8) into Eq. (2), we have

$$\frac{k_e}{k_f} = 1-\frac{\pi}{4}+\frac{\pi}{8}\left\{A(1+A)+(1-A^2)(1+\sqrt{1-A^2})\beta-(1-A+3\sqrt{1-A^2})\frac{1}{\beta}\right.$$
$$\left.-\frac{1}{\beta^2} ln[(1-\beta+\beta A)(1-\beta\sqrt{1-A^2})^3]+\beta^2(1-A^2)^2 ln\left[\sqrt{\frac{1+A}{1-A}}\frac{1-\beta(1-A)}{1-\beta\sqrt{1-A^2}}\right]\right\} \tag{10}$$

This is the effective thermal conductivity expression based on the point-contact hollow spherical model without radiation. Obviously, this effective thermal conductivity is dependent on the thermal conductivity of the solid, the thermal conductivity of the fluid, and the microstructure of the xonotlite as well as the porosity of the shell.

3. SURFACE-CONTACT HOLLOW CUBIC MODEL

3.1. Geometrical Structure

Actually, spherical agglomerates in xonotlite are not in perfect point contact, and there exists some contact area between them. We can consider xonotlite as an array of hollow cubic structures with a side length a, and a wall thickness h. Hollow cubic structures are in contact through a section $c \times c$ as shown in Fig. 3a.

The following dimensionless parameters can be defined similarly in the literature [11]:

$$\gamma_a = a/l, \qquad \gamma_b = 2h/a, \qquad \gamma_c = c/a \tag{11}$$

The porosity of the unit cell is as follows:

$$\Phi = 1 - (1 - \Phi_i)[(1 - (1 - \gamma_b)^3 - 3\gamma_c^2)\gamma_a^3 + 3\gamma_a^2\gamma_c^2] \tag{12}$$

3.2. Effective Thermal Conductivity

The one-dimensional heat conduction, as shown in Fig. 3b, is considered. As discussed above, conduction in a unit cell consists of four parts (see Fig. 4): (I) transferred through rectangular shape $(l-a)/2 \times l/2 \times l/2$, (II) through rectangular shape $h \times l/2 \times l/2$; (III) through rectangular shape $(a-2h-c)/2 \times l/2 \times l/2$, and (IV) through rectangular shape $c/2 \times l/2 \times l/2$. Therfore, the effective thermal conductivity of the unit cell is

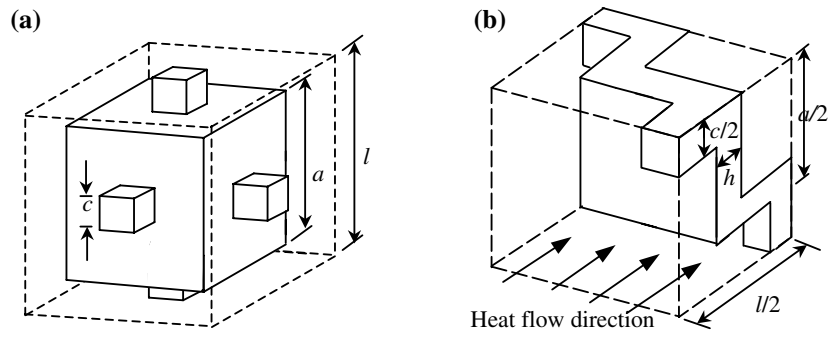

Fig. 3. Surface-contact hollow cubic structure and unit cell model of xonotlite. (a) Surface-contact hollow cubic structure and (b) Unit cell.

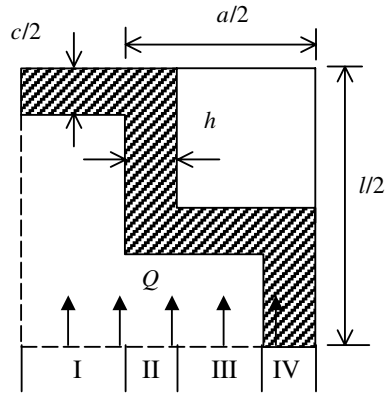

Fig. 4. Unit cell in plane view.

$$k_e = (1-\gamma_a)k_{sf1} + \gamma_a\gamma_b k_{sf2} + \gamma_a(1-\gamma_b-\gamma_c)k_{sf3} + \gamma_a\gamma_c k_{sf4} \tag{13}$$

where k_{sf1}, k_{sf2}, k_{sf3}, and k_{sf4} are the effective thermal conductivities corresponding to parts (I), (II), (III), and (IV), respectively. The corresponding expressions for k_{sf1}, k_{sf2}, k_{sf3}, and k_{sf4} are

$$k_{sf1} = \frac{\gamma_a\gamma_c k_f k_c}{(1-\gamma_a\gamma_c)k_c + k_f\gamma_a\gamma_c} + (1-\gamma_a\gamma_c)k_f \tag{14}$$

$$k_{sf2} = \frac{\gamma_a k_f k_c}{(1-\gamma_a)k_c + k_f\gamma_a} + (1-\gamma_a)k_f \tag{15}$$

$$k_{sf3} = \frac{\gamma_a(1-\gamma_b)k_f k_c}{(1-\gamma_a\gamma_b)k_c + k_f\gamma_a\gamma_b} + \frac{\gamma_a\gamma_b k_f k_c}{(1-\gamma_a)k_c + k_f\gamma_a} + (1-\gamma_a)k_f \tag{16}$$

$$k_{sf4} = \frac{\gamma_a(1-\gamma_b-\gamma_c)k_f k_c}{(1-\gamma_a\gamma_b)k_c + k_f\gamma_a\gamma_b} + \frac{\gamma_a\gamma_b k_f k_c}{(1-\gamma_a)k_c + k_f\gamma_a} + \frac{(1-\gamma_a)k_f k_c}{(1-\gamma_a\gamma_c)k_c + k_f\gamma_a\gamma_c} + \frac{\gamma_a\gamma_c k_f k_c}{(1-\gamma_a+\gamma_a\gamma_b)k_f + k_c\gamma_a(1-\gamma_b)} \tag{17}$$

where k_f and k_c are the thermal conductivities of the fluid and shell, respectively. Substituting Eqs. (14) to (17) into Eq. (13), we have

$$\frac{k_e}{k_f} = \frac{(2-\gamma_b)\gamma_a^2\gamma_b}{1-(1-\beta)\gamma_a} + \frac{\gamma_a^2[(1-\gamma_b)^2-\gamma_c^2]}{1-(1-\beta)\gamma_a\gamma_b} + \frac{2\gamma_a\gamma_c(1-\gamma_a)}{1-(1-\beta)\gamma_a\gamma_c} + \frac{\gamma_a^2\gamma_c^2}{\beta+(1-\beta)(1-\gamma_b)\gamma_a} + (1-\gamma_a)(1+\gamma_a-2\gamma_a\gamma_c) \tag{18}$$

This is the effective thermal conductivity expression based on the surface-contact hollow cubic model without radiation. Obviously, this effective thermal conductivity is also dependent on the thermal conductivity of the solid, the thermal conductivity of the fluid, and the microstructure of the xonotlite as well as the porosity of the shell.

4. TERM FOR RADIATION HEAT TRANSFER

Radiation heat transfer is another important heat transfer mechanism in porous insulation materials. At high temperatures thermal radiation can be very large and cannot be neglected. In practical applications, the optical thickness of insulators is typically very large. For an optically thick medium, radiation travels only a short distance. The local intensity is the result of radiation from nearby locations only. The energy transfer depends only on the conditions in the intermediate vicinity of the position being considered. For the two models of this study, the thermal radiation formula from the Loeb model is adopted, in which radiation heat transfer in the unit cell is divided into two parts: thermal radiation occurring inside the hollow spherical shell and outside the hollow spherical shell. They are both added into the part of the thermal conductivity of the fluid in the unit cell. The thermal radiation formula is [15]

$$k_r = 4Gd\varepsilon\sigma T^3 \tag{19}$$

Here, G is the shape factor of a pore (for a spherical pore, $G=2/3$, and for a rectangular pore, $G=1$), d is the maximum dimension of a pore in the heat flow direction, ε is the emissivity of the radiation surface, σ is the Stefan–Boltzmann constant, and T is the average absolute temperature of a pore.

5. EFFECTIVE THERMAL CONDUCTIVITY OF THE SHELL k_c

The shell of xonotlite secondary particles is formed by interwoven xonotlite fibers. Some pores also exist in the shell. Here, we adopt the parallel model [12] to estimate the effective thermal conductivity of the shell,

k_c, which is

$$k_c = \Phi_i k_f + (1 - \Phi_i) k_s \tag{20}$$

where k_s is the thermal conductivity of the xonotlite fibers and Φ_i is the porosity of the shell.

6. RESULTS AND DISCUSSION

Figure 5 shows comparisons of experimental data [2, 3, 16] with the best fits of the point-contact hollow spherical model and the surface-contact hollow cubic model ($\gamma_a = 0.78$ and $\gamma_c = 0.1$). In the calculations, the thermal conductivity of air is $k_f = 0.026\,\mathrm{W \cdot m^{-1} \cdot K^{-1}}$, and the thermal conductivity of the xonotlite fibers $k_s = 1.8\,\mathrm{W \cdot m^{-1} \cdot K^{-1}}$. According to the literature [3], the thickness of the shell $h = 4\mu\,\mathrm{m}$ and the porosity of the shell $\Phi_i = 0.8$ are adopted for the two unit cell structures. It is shown that the results based on the surface-contact hollow cubic model agree with experimental data better than the point-contact hollow spherical model, although the differences between the two models and between the models and experimental data are within 10%. The results based on the point-contact hollow spherical model are a little lower than those based on the surface-contact hollow cubic model. This difference may be explained by the fact that hollow spherical agglomerates are not in perfect point contact, i.e., there is some surface contact between them. The surface-contact hollow cubic structure is likely a more reasonable representation of the real microstructure of xonotlite, and the model based on this kind of structure can be used to more accurately estimate the thermal conductivity.

As mentioned above, radiation heat transfer is another important heat transfer mechanism in porous insulation materials. Figure 6 shows the effect of temperature on the effective thermal conductivity of xonotlite based on the two models. It is shown that some differences exist between the two models and the linear relationship mentioned in the literature [16]. It is considered that the results of our models are more reasonable because the cubic relationship exists between the radiative thermal conductivity and temperature, $k_r \sim T^3$.

7. CONCLUDING REMARKS

The concept of a unit cell model for a periodic medium has been widely used in other physical problems, such as electrical conductivity, micromechanics, permeability, etc. Some effective thermal conductivity models based on the unit cell structure have also been developed previously

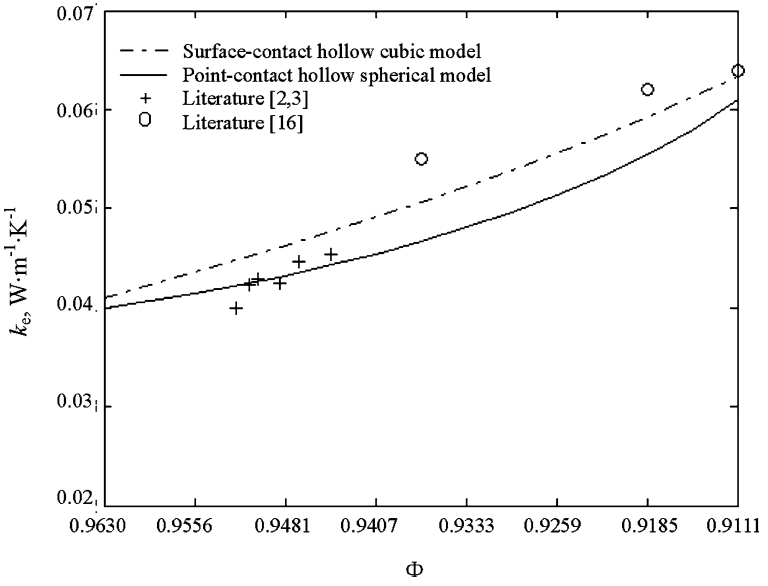

Fig. 5. Comparison of effective thermal conductivity of models with experimental data.

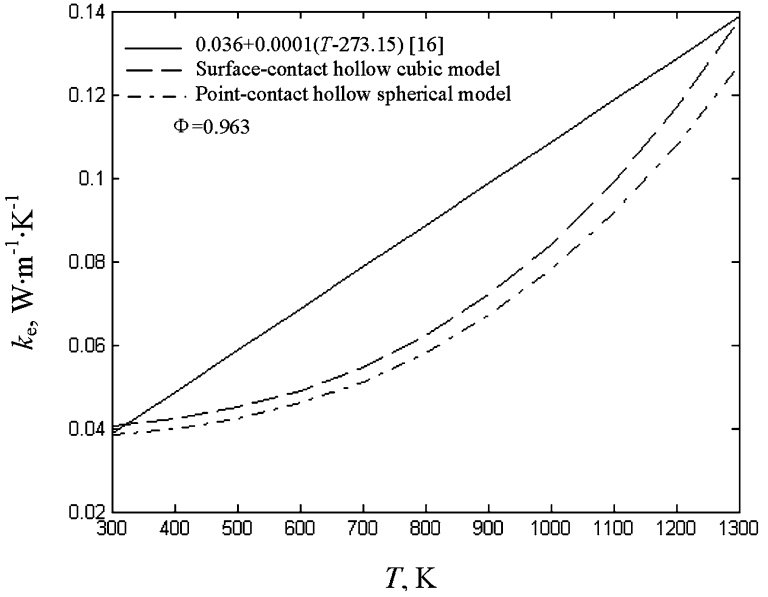

Fig. 6. Effect of temperature on the effective thermal conductivity of xonotlite.

for porous media [8–11, 17]. However, those models cannot be used to calculate the effective thermal conductivity of xonotlite-type micro-pore calcium silicate directly because of its high porosity (> 90%) and peculiar structure features (hollow spherical agglomerates). Based on the microstructure features of xonotlite, two unit cell models, the point-contact hollow spherical model and the surface-contact hollow cubic model, have been developed. Expressions for the effective thermal conductivity have been derived. It is shown that the differences between the two models and experimental data in the literature are within 10%, and that the effective thermal conductivity based on the surface-contact cubic model agrees better with experimental data.

8. ACKNOWLEDGMENT

This research was financially supported by the National Natural Science Foundation of China (No. 50276003).

REFERENCES

1. S. White and D. Rask, *Mater. Technol*. **14**:13 (1999).
2. M. Q. Li, Y. F. Chen, S. Q. Xia, J. H. Li, and H. X. Ling, *J. Chinese Ceramic Soc*. **28**:401 (2000). [in Chinese]
3. Q. J. Zheng and W. Wang, *New Build. Mater*. **10**:25 (2000). [in Chinese]
4. Z. Y. Wang, Y. M. Huang, M. M. Wu, and G. Q. Xue, *Naihuo Cailiao* **31**:134 (1997). [in Chinese]
5. W. Ni and F. M. Liu, *New Build. Mater*. **1**:36 (2000). [in Chinese]
6. P. J. Burns and C. L. Tien, *Int. J. Heat Mass Transfer* **22**:929 (1979).
7. T. G. Xi, *A Study on Thermophysical Properties of Inorganic Material* (Shanghai Science and Technology Press, Shanghai, 1981). [in Chinese]
8. P. Zehnder and E. U. Schlunder, *Chem. Ingr.-Tech*. **42**:933 (1970). [in German]
9. R. W. Zimmerman, *J. Petrol. Sci. Eng*. **3**:219 (1989).
10. L. S. Verma, A. K. Shrotriya, R. Singh, and D. R. Chaudhary, *J. Phys. D*. **24**:1729 (1991).
11. C. T. Hsu, P. Cheng, and K. W. Wong, *J. Heat Transfer* **177**:264 (1995).
12. B. M. Yu and P. Cheng, *J. Thermophys. Heat Transfer* **16**:22 (2002).
13. Y. T. Ma, B. M. Yu, D. M. Zhang, and M. Q. Zou, *J. Phys. D* **36**:2157 (2003).
14. Y. J. Feng, B. M. Yu, M. Q. Zou, and D. M. Zhang, *J. Phys. D* **37**:3030 (2004).
15. A. L. Loeb, *J. Am. Ceram. Soc*. **37**:96 (1954).
16. L. J. Mo, Z. H. Wang, and X. H. Liu, *A Handbook of Insulating Engineering and Technology* (Chinese Petrochemical Press, Beijing, 1997). [in Chinese]
17. A. E. Saez, J. C. Perfetto, and L. Rusinek, *Trans. Porous Media* **6**:143 (1991).